Chinese Chemical Letters 32 (2021) 1046–1050

Contents lists available at ScienceDirect

Chinese Chemical Letters

journal homepage: www.elsevier.com/locate/cclet

Communication

Reduction-sensitive nanomicelles: Delivery celastrol for retinoblastoma cells effective apoptosis

Zhihua Guo[a,1], Liuqi Shi[a,b,1], Huayang Feng[a,b], Fan Yang[a], Zhanrong Li[a,**], Junjie Zhang[a], Lin Jin[a], Jingguo Li[a,b,*]

[a] Henan Eye Hospital, Henan Provincial People's Hospital, Zhengzhou University People's Hospital, Zhengzhou 450003, China
[b] School of Materials Science and Engineering, Zhengzhou University, Zhengzhou 450001, China

ARTICLE INFO

Article history:
Received 20 January 2020
Received in revised form 23 March 2020
Accepted 24 March 2020
Available online 4 April 2020

Keywords:
Reduction-sensitive
Nanomicelles
Retinoblastoma
Celastrol
Cell apoptosis

ABSTRACT

Celastrol, a Chinese herbal medicine, has exhibited anticancer activity in many types of cancer cells. However, the further clinical application of celastrol is restricted by its poor water solubility and serious side effects. Furthermore, the apoptosis mechanism of tumor cells induced by celastrol has not been exhausted yet. In this study, we developed a reduction sensitive polymeric vector for tumor-targeted celastrol delivery. And our researches indicated that the celastrol could be delivered by reduction-sensitive nanomedicine (RSNMs) with a controlled release strategy. Meanwhile, the cell uptake results indicated that excellent reduction-sensitive behavior of RSNMs could effectively accelerate celastrol into the human retinoblastoma (RB) cell. The cell cytotoxicity assay demonstrated that celastrol inhibited proliferation of human RB Y79 cells growth in a dose-dependent manner. Furthermore, the results of flow cytometry and terminal dUTP nick-end labeling (TUNEL) staining showed that celastrol induced apoptosis of the RB Y79 cells, and revealed a time-dependent increase in apoptosis induction of RB Y79 cells. The results of western blotting showed that celastrol induced the apoptosis of human RB Y79 cells involving the activation of caspase-3 and caspase-9. In conclusion, our results revealed that RSNMs may be utilized as a novel therapy for retinoblastoma.

Retinoblastoma (RB) is the primary intraocular malignancy of childhood, with a constant incidence of 1 in 15,000–20,000 live births [1]. The therapy of curing RB is multimodal, including enucleation, chemotherapy and focal treatments (such as laser photocoagulation, brachytherapy and transpupillary thermotherapy) [2,3]. Primary enucleation is a simple straightforward standard therapy to cure the patients. However, it may lead to vision loss and an unsatisfactory cosmetic appearance. In recent years, chemotherapy was used as the main treatment choice for RB [4]. Therefore, developing potential therapeutic drugs and corresponding delivery vectors to induce RB cells apoptosis has become a critical research domain of RB investigations.

Celastrol is a pentacyclic triterpene with anti-tumor [5], anti-inflammatory [6], anti-angiogenesis [7], and antiobesity potentials [8]. Celastrol could induce apoptosis of human multiple myeloma [9], desmoplastic melanoma [5] and nasopharyngeal carcinoma [10]. Our previous study has demonstrated that celastrol could suppress the growth of retinoblastoma in a mouse xenograft model by inducing the apoptosis of human retinoblastoma SO-Rb 50 cells [11]. In previous research, celastrol nanomicelles could suppress angiogenesis-mediated retinoblastoma growth [12]. Nevertheless, the further clinical applications of celastrol are greatly restricted by its poor water solubility. Normally, utilizing the polymer on the basis of self-assemblies as vectors to delivery low water solubility drug into tumor is an effective strategy to enhance the effectiveness [13,14].

Stimuli-responsive polymeric vectors and nanomedicines have been designed to delivery and release drugs in response to an appropriate stimulation such as change in glutathione (GSH), pH or temperature [15]. For example, utilizing the GSH concentration difference between the extracellular (20–40 μmol/L) and intracellular (1–10 mmol/L), reduction-sensitive systems have been

* Corresponding author at: Henan Eye Hospital, Henan Provincial People's Hospital, Zhengzhou University People's Hospital, Zhengzhou 450003, China.
** Corresponding author.
E-mail addresses: lizhanrong@zzu.edu.cn (Z. Li), lijingguo@zzu.edu.cn (J. Li).
[1] These authors contribute equally to this work.

https://doi.org/10.1016/j.cclet.2020.03.066
1001-8417/

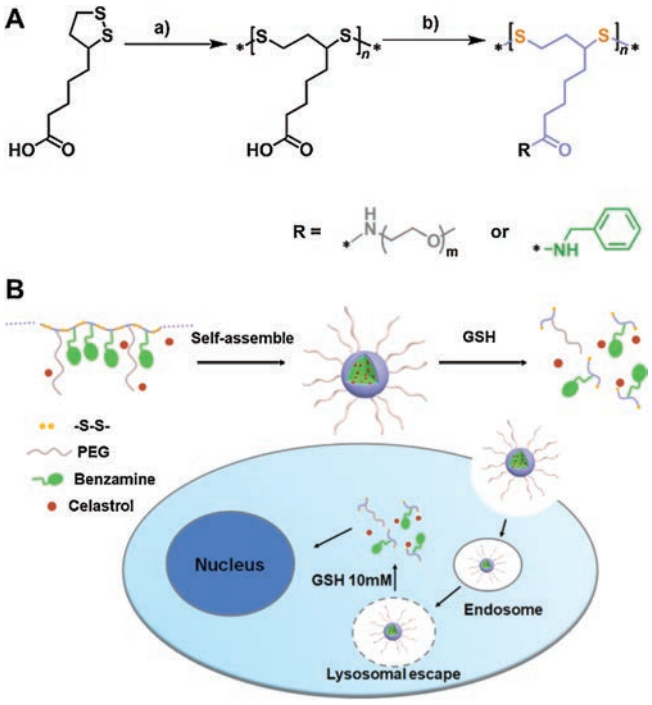

Fig. 1. (A) Synthesis route of PTEB; (B) Schematic illustration of the RSNMs formation, internalization into cancer cells and intracellular celastrol release.

developed to achieve tumor-targeted drug delivery [16,17]. Herein, a novel polymeric vector with high density disulfide-containing in the backbone chain was prepared to reduction-sensitive nanomedicine (RSNMs) for tumor-targeted celastrol delivery (Fig. 1) [18]. *In vitro* investigations demonstrated that RSNMs have more advantages in inducing the apoptosis of the human RB cells than small molecule celastrol itself, expanding the potential applications of celastrol in the treatment of tumor. First of all, the reduction-sensitive grafted copolymer poly[thioctic acid-grafted-poly(ethylene glycol)/(benzyl amine)], denoted as PTEB, was synthesized by self-polymerization of thioctic acid and subsequent amidation reaction of thioctic acid (TA) with PEG and benzyl amine (BA) outlined in Fig. 1A. The polymer was characterized by ^{1}H NMR and the corresponding structure is shown in Fig. 2A. After grafting PEG and BA onto PTA, the new resonance peak at δ 3.51, 4.25 and 7.24 were attributed to PEG and BA, respectively, suggesting the successful synthesis of PTEB.

Next, the size and morphology of blank PTEB micelles (B-PTEB) in aqueous solution were characterized *via* DLS and TEM, and the results indicated the B-PTEB have a relatively small average hydrodynamic diameter of 69 ± 3 nm (Fig. 2D) indicating their uniform spherical shape (Fig. 2B). The celastrol loading content of celastrol-loaded PTEB micelle (C-PTEB) was 8.51% determined by HPLC (Fig. S1 in Supporting information).

To qualitatively verify the reduction-sensitive drug release properties of RSNMs *in vitro*, the fluorescein diacetate (FDA) release studies of FDA-loaded micelle (F-PTEB) and the change of particle size of B-PTEB were investigated in lysosome-mimicking environment. As shown in Fig. 2C, the quantitatively measurement of FDA fluorescence emission of F-PTEB in solution clearly showed the reduction-sensitive FDA release behavior of RSNMs. FDA fluorescence intensity was very low at normal physiological environment. In comparison, FDA fluorescence intensity significantly increased at lysosomal reduction environment. As shown in Fig. 2D, the particle size of RSNMs determined by DLS measurement changed from 70 nm to 1480 nm and the size polydispersity changed from 0.245 to 0.531, which further evidenced the reduction-sensitive behavior. These results indicated that RSNMs have an excellent reduction-sensitive behavior and would break disulfide bonds in polymer chain under lysosomal reduction environment.

Cell uptake of C-PTEB was evaluated with confocal laser scanning microscopy (CLSM) (Fig. 3A). The results showed that

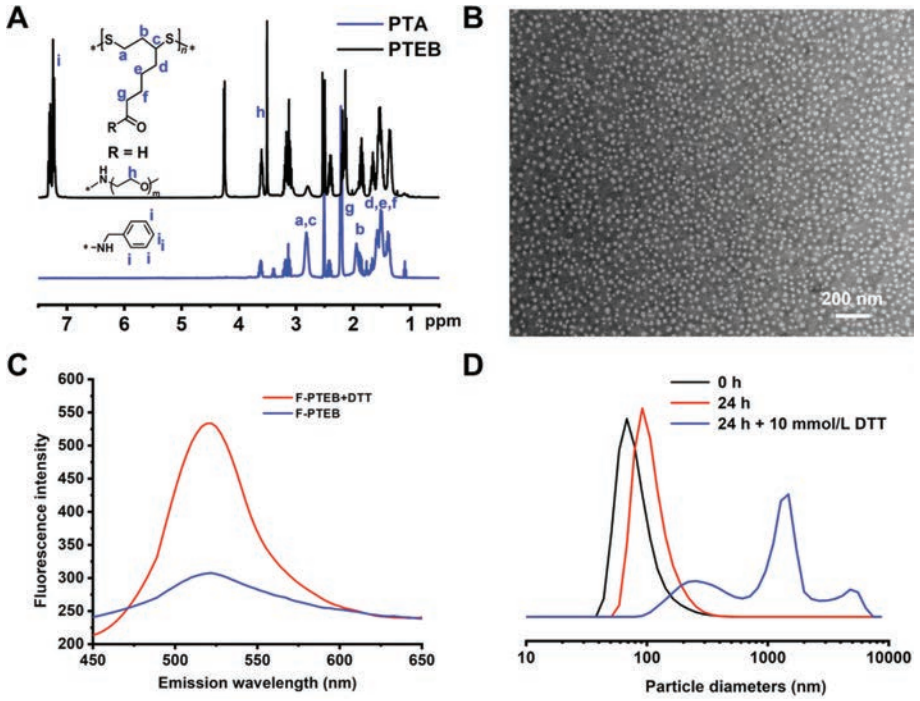

Fig. 2. (A) ^{1}H NMR spectra of PTA and PTEB; (B) TEM of PTEB micelles in H_2O; (C) Fluorescence intensity comparison of F-PTEB with or without DTT; (D) The diameter changes of RSNMs under different conditions.

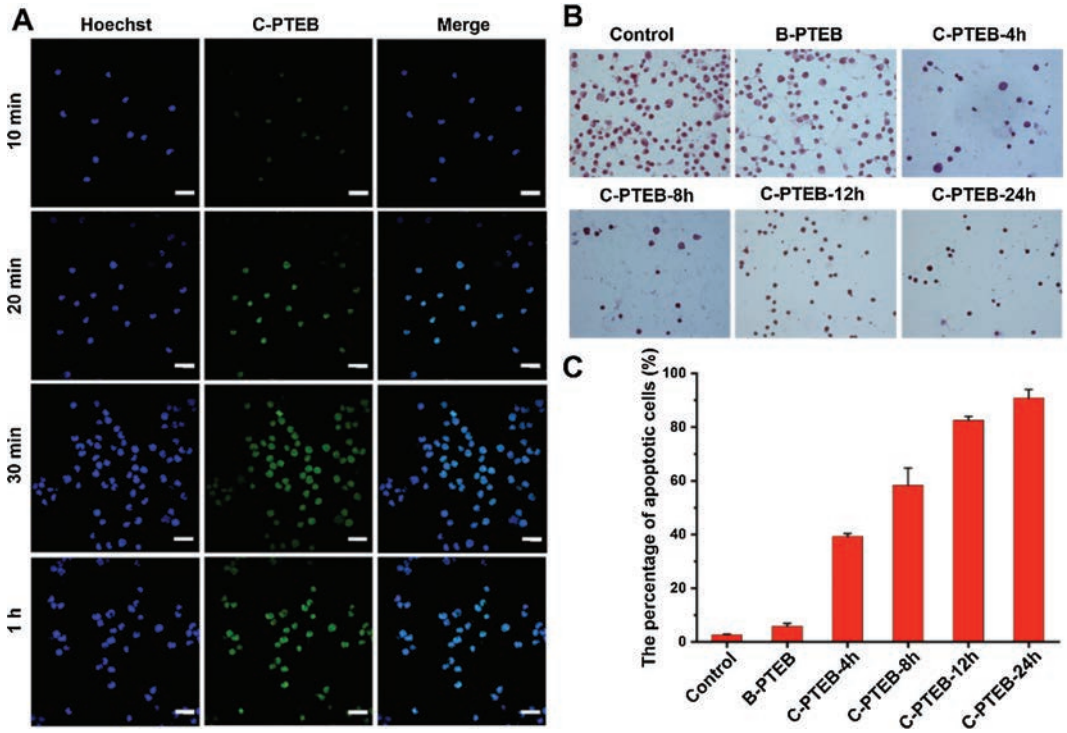

Fig. 3. (A) Confocal laser microscopic images of Y79 cells incubated with C-PTEB at different time points. Green fluorescence: celastrol; blue fluorescence: nuclei stained with Hoechst. The scale bar is 20 μm. The apoptosis of Y79 cells was evaluated by TUNEL assay (B) and statistical apoptosis rate (C).

green fluorescence was observed in the Y79 cells just in 10 min after cells were incubated with C-PTEB. Moreover, with the extension of time, more celastrol migrated to the nuclear from cytoplasm. After incubation for 1 h, strong green fluorescence of celastrol was only observable in nuclear of Y79 cells. These results indicated that the reduction-sensitive drug release properties of C-PTEB contribute to rapid-release of celastrol from C-PTEB inside the cell, and the process of migration into the nuclear.

The cells proliferation inhibition effects of C-PTEB in Y79 cells were detected using Cell Counting Kit-8 (CCK8) assay. At various concentrations of C-PTEB (celastrol, 2.66, 5.32, 10.64, 21.28, 42.56 and 85.12 μg/mL), the viability of Y79 cells decreased obviously (Fig. S2 in Supporting information). The Y79 cells were treated with various concentrations of B-PTEB (31.25, 62.5, 125, 250 and 500 μg/mL), and the results showed that B-PTEB have no toxicity for the Y79 cells (Fig. S3 in Supporting information).

TUNEL assay confirmed the apoptosis induction of C-PTEB on Y79 cells. As shown in Figs. 3B and C, the nucleus of the apoptotic Y79 cells were stained dark brown. With prolongation of the time of C-PTEB action (celastrol, 8.51 μg/mL), the rate of apoptosis of Y79 cells showed an increasing trend. And under action time (12 and 24 h), most of the Y79 cells were dead. Moreover, apoptosis of Y79 cells treated with C-PTEB was detected by the PE-annexin V/7-AAD staining and analyzed by flow cytometry (FCM). The results of FCM revealed that the early apoptosis and late apoptosis rates of the 4, 8, 12 and 24 h C-PTEB (celastrol, 8.51 μg/mL) groups were all higher than the control group and B-PTEB group (Figs. 4A and B; $P < 0.05$). Furthermore, celastrol can induce apoptosis of Y79 cells, including the early apoptosis and the late apoptosis, increased with the prolongation of drug time. These results indicated that celastrol could induce apoptosis of the RB Y79 cells.

Western blotting results showed that after treating Y79 cells with C-PTEB (celastrol, 1.70 μg/mL) for 12 h, the expression levels of caspase-related proteins (caspase-3, caspase-9) were all increased, while caspase-8 has not changed much compared to the control group (Figs. 4C and D; $P < 0.01$). These results indicated that effector caspase-3 and caspase-9 were activated in RB Y79 cells apoptosis induced by celastrol.

In the present study, our results of cell uptake of C-PTEB (Fig. 3A) have demonstrated that excellent reduction-sensitive behavior of C-PTEB could effectively accelerate celastrol into the human retinoblastoma cell and result in better effect under internal reduction environment. And the CCK8 assay demonstrated that celastrol inhibited the proliferation of RB Y79 cells with just 4 h at concentration of celastrol (2.66, 5.32, 10.64, 21.28, 42.56 and 85.12 μg/mL) (Fig. S2).

Apoptosis is a mechanism which is crucial to maintain a healthy balance of cell proliferation and cell death [19,20]. Our previous research demonstrated that celastrol-loaded nanomicelles can significantly inhibit activity of human retinoblastoma SO-Rb 50 cells, meanwhile, suppress the growth of retinoblastoma in a xenograft mouse model through inducing the apoptosis of RB cells [9]. The results of flow-cytometric analyses (Figs. 4A and B) in this study have showed that celastrol induced apoptosis of the RB Y79 cells, and revealed a time-dependent increase in apoptosis induction in RB Y79 cells treated with C-PTEB (celastrol, 8.5 μg/mL). This observation was further confirmed by TUNEL staining (Figs. 3B and C), with an increasing number of TUNEL-positive cells in C-PTEB-treated groups as time progressed. And the number of apoptotic cells in C-PTEB-treated groups was more than the control group. These results demonstrated that celastrol can be a potential alternative therapy for RB.

As is known to all, caspase-3 is executioner caspase, and initiator caspases (caspase-8, caspase-9) are the apical caspases of the apoptotic-signaling cascade. Additionally, caspase-9 involved in the mitochondrial pathway of apoptosis (also called the intrinsic pathway) [21]. Moreover, caspase-8 is activated predominantly by the death receptor pathway of vertebrate apoptosis [22]. Chen *et al.*, found that celastrol could induce apoptosis of multiple

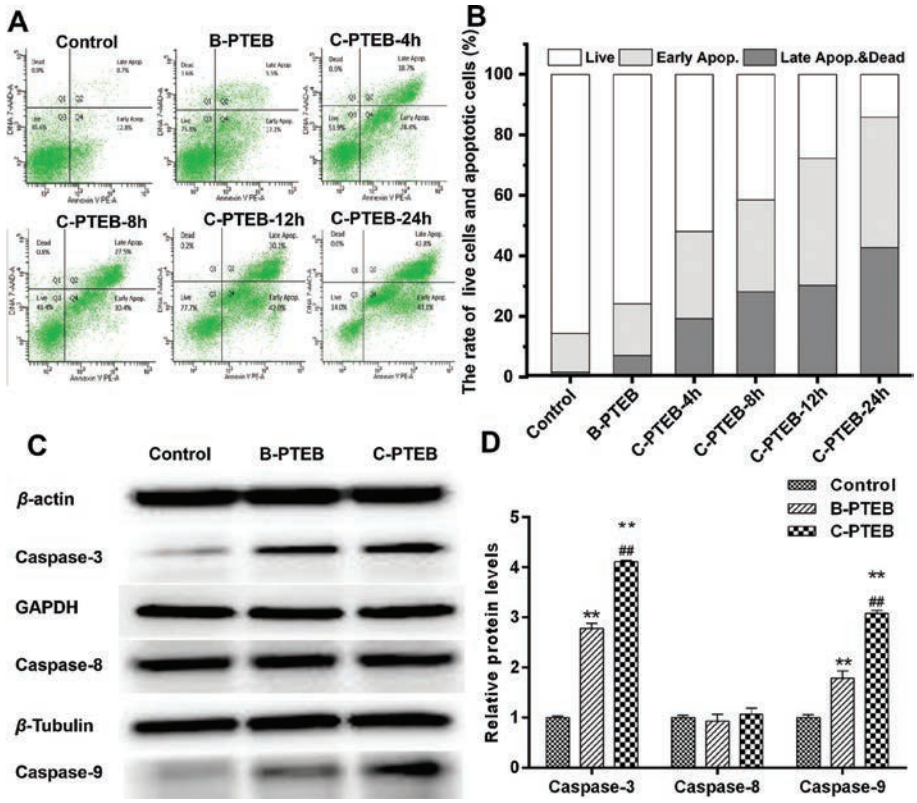

Fig. 4. C-PTBA induced apoptosis of Y79 cells. (A) The apoptotic rates at different time-points (4, 8, 12 and 24 h) were analyzed with FCM. (B) Statistics of the proportion of living, early apoptosis and late apoptosis rates in different groups. C-PTEB activated caspase 3 and caspase 9 in involved apoptosis in Y79 cells (C and D). At 12 h following treatment, whole-cell lysates were prepared to assay caspase-3, caspase-8, and caspase-9 proteins by western blotting. Data are presented as the mean ± SD from three independent experiments. $^{**}P < 0.01$, compared with the control group. $^{\#\#}P < 0.01$, compared with the B-PTEB group.

osteosarcoma HOS cells and promote the expression of apoptosis-related proteins (cytochrome c, cleaved caspase-12, cleaved caspase-3) [23]. Meanwhile, an increase in cleaved form of caspase-3 in multiple myeloma U266 cells treated with a combination of celastrol and bortezomib was also found to be significantly higher than celastrol or alone treated cells [24–26]. In the results of western blotting (Figs. 4C and D), we found that celastrol can significantly improve the expression levels of caspase-related proteins (caspase-3, caspase-9) in Y79 cells treated with C-PTEB (celastrol, 1.70 μg/mL). Finally, this study revealed that celastrol could induce apoptosis of RB Y79 cells, and up-regulate the expression of caspase-3 and caspase-9 in RB Y79 cells treated with C-PTEB. These results will provide a basis for the future research of celastrol as a novel therapy for the treatment of RB.

In summary, a reduction responsive nanomedicine system basing on disulfide-containing block copolymer and celastrol was successfully developed in this study. The results of TUNEL staining and flow-cytometric analyses in this study have showed that celastrol induced apoptosis of RB Y79 cells and revealed a time-dependent increase in apoptosis induction in RB Y79 cells treated with C-PTEB. The results demonstrated that celastrol could be delivered by RSNMs with a controlled release strategy in responsive with the reduction micro-environment inside of tumor, subsequently suppress proliferation of human RB Y79 cells and induce apoptosis of human RB Y79 cells. Furthermore, we also found that celastrol induce apoptosis of human RB Y79 cells involving the activation of caspase-9 and caspase-3. Our results demonstrated that celastrol in our system could represent as a novel therapy for retinoblastoma.

Declaration of competing interest

The authors declare that they have no known competing financial interests or personal relationships that could have appeared to influence the work reported in this paper.

Acknowledgments

This research was supported by the National Natural Science Foundation of China (Nos. 81600775, U1904176 and 21504082), the Science and Technology Program of Henan Province, China (No. 202102310072), the Medical Science and Technology Program of Henan Province, China (Nos. 2018020398 and SB201902026).

Appendix A. Supplementary data

Supplementary material related to this article can be found, in the online version, at doi:https://doi.org/10.1016/j.cclet.2020.03.066.

References

[1] I.D. Fabian, Z. Onadim, E. Karaa, et al., Oncogene 37 (2018) 1551–1560.
[2] A. Maheshwari, P.T. Finger, Cancer Metastasis Rev. 37 (2018) 677–690.
[3] C.L. Shields, E.M. Fulco, J.D. Arias, et al., Eye 27 (2013) 253–264.
[4] H. Zhang, B. Li, S.W. Bai, et al., Cancer Invest. 28 (2010) 156–165.
[5] Q. Liu, F. Chen, L. Hou, et al., ACS Nano 12 (2018) 7812–7825.
[6] L. Guo, S. Luo, Z. Du, et al., Nat. Commun. 8 (2017) 878.
[7] Z. Li, L. Yao, J. Li, et al., Int. J. Nanomedicine 7 (2012) 1163–1173.
[8] X. Feng, D. Guan, T. Auen, et al., Nat. Med. 25 (2019) 575–582.
[9] Y. Zhong, G. Xu, S. Huang, et al., Eur. J. Pharmacol. 853 (2019) 184–192.
[10] H.F. Lin, M.J. Hsieh, Y.T. Hsi, et al., Oncol. Lett. 14 (2017) 1683–1690.

[11] Z. Li, X. Wu, J. Li, et al., Int. J. Nanomedicine 7 (2012) 2389–2398.
[12] Z. Li, Z. Guo, D. Chu, et al., Drug Deliv. 1 (2020) 358–366.
[13] Y. Sun, W. Ma, Y. Yuan, et al., Asian J. Pharm. Sci. 14 (2019) 581–698.
[14] W. Sui, N. Pei, L. Chen, et al., Adv. Healthc. Mater. 1 (2020) e1901100.
[15] J. Li, L. Zhang, Y. Lin, et al., RSC Adv. 6 (2016) 9160–9163.
[16] J. Li, X. Yu, Y. Wang, et al., Adv. Mater. 26 (2014) 8217–8224.
[17] D. Natasha, Sheybani, H. Yang, Chin. Chem. Lett. 28 (2017) 1817–1821.
[18] Y.F. Zhou, X. Li, Chin. Chem. Lett. 28 (2017) 1835–1840.
[19] H.L. Jiang, J.Z. Jin, D. Wu, et al., Mol. Biol. Rep. 40 (2013) 4203–4209.
[20] S. Goldar, M.S. Khaniani, S.M. Derakhshan, et al., Asian Pac. J. Cancer Prev. 16 (2015) 2129–2144.
[21] S.B. Bratton, G.S. Salvesen, J. Cell. Sci. 123 (2010) 3209–3214.
[22] L.S. Dickens, I.R. Powley, M.A. Hughes, et al., Exp. Cell Res. 318 (2012) 1269–1277.
[23] Y. Chen, Y. Ou, Y. Tao, et al., Oncol. Rep. 40 (2018) 2260–2268.
[24] M.K. Shanmugam, K.S. Ahn, J.H. Lee, et al., Front. Pharmacol. 9 (2018) 365.
[25] Y. Wang, X. Wang, J. Zhang, et al., Chin. Chem. Lett. 30 (2019) 885–888.
[26] Q. Zhang, C.Y. Shi, D.H. Qu, et al., Sci. Adv. 4 (2018) eaat8192.